Article

Enzymatic Biofuel Cell Based Self-Powered Biosensor Integrated with DNA Amplification Strategy for Ultrasensitive Detection of Single-Nucleotide Polymorphism

Chengcheng Gu, Xinke Kong, Xiaojuan Liu, Panpan Gai, and Feng Li

Anal. Chem., **Just Accepted Manuscript** • DOI: 10.1021/acs.analchem.9b02510 • Publication Date (Web): 06 Jun 2019

Enzymatic Biofuel Cell Based Self-Powered Biosensor Integrated with DNA Amplification Strategy for Ultrasensitive Detection of Single-Nucleotide Polymorphism

Chengcheng Gu, Xinke Kong, Xiaojuan Liu, Panpan Gai* and Feng Li*

College of Chemistry and Pharmaceutical Sciences, Qingdao Agricultural University, Qingdao 266109, P. R. China.

*Corresponding authors: Tel/Fax: 86-532-86080855;

E-mail: lifeng@qau.edu.cn

ABSTRRACT

Enzymatic biofuel cells (EBFCs)-based self-powered biosensor could offer significant advantages in no requirement of external power source, simple instruments and easy miniaturization. However, they also suffered from the limitations of lower sensitivity or specific targets. In this study, a self-powered biosensor for the ultrasensitive and selective detection of single nucleotide polymorphisms (SNPs) via combining the toehold-mediated strand displacement reaction (SDR) and DNA hybridization chain reaction (HCR) was proposed. Herein, the capture probe (CP) with an external toehold was designed to switch on the sensing system. In the presence of target sequence, both SDR and DNA HCR reaction would happen to produce a long double-helix chain. Owing to the electrostatic interaction between more $[Ru(NH_3)_6]^{3+}$ and the above double-helix chain, the open circuit voltage (E^{OCV}) of the as-proposed biosensor was significantly elevated, thus realizing the detection of SNPs. Overall, this work ingeniously constructed self-powered biosensor for the detection of SNPs by integrating EBFCs with DNA amplification strategy. Furthermore, the as-proposed self-powered biosensor not only showed prominent specificity to distinguish the p53 gene fragment from random sequences (e.g., single-base mutant sequences), but exhibited excellent sensitivity with the detection limit of 20 aM. More importantly, the satisfied results obtained from the cell lysate real sample have laid strong foundation for disease diagnostics and ever more fields as a powerful tool.

INTRODUCTION

Enzymatic biofuel cells (EBFCs) have received considerable attentions because of the intrinsic capability to directly produce electrical energy from renewable biomass or biofuels, as well as some promising applications, such as implantable power sources and self-powered biosensors.[1, 2] In comparison with the traditional biosensors, self-powered biosensors exhibited some unique advantages of no requirement of external power source, simple instruments and easy miniaturization.[3-5] Up to date, the self-powered biosensors based on EBFCs as powerful strategies have been widely applied in cytosensing,[6-8] immunoassays[9-11] as well as the detection of molecules[12-14] and toxic pollutants[15]. Among them, a series of self-powered design principles of inhibition effect, blocking effect, substrate effect and enzyme activity combined with the biorecognition techniques including biofuel-enzyme, antibody-antigen, and aptamer-protein were developed. [5, 9, 16, 17] For example, Zhu et al. reported an EBFCs-based self-powered cytosensor for acute leukemia CCRF-CEM cells detection through the blocking effect and biorecognition technique, which exhibited excellent anti-fouling ability and could be in favor of the biosensor miniaturization for vivo application.[7] In spite of the achieved progress, the evolution of EBFCs-based self-powered biosensing platforms still suffered from the limitations of lack of the effective signal amplification strategy, relatively low sensitivity or specific targets. Thus, how to develop the signal amplification strategy is crucial for the wide application of self-powered biosensors.

DNA amplification strategy is attractive because of the structures diversity via ingenious design, which contains hybridization chain reaction (HCR), rolling circle amplification (RCA) as well as polymer chain reaction (PCR) and so on. As we know, DNA amplification strategy generally contains nonenzyme-mediated amplification method (e.g., hybridization chain reaction, HCR) and enzyme-mediated cycling amplification, such as rolling circle amplification (RCA), polymer chain reaction (PCR).[18-21] Apart from them, strand displacement reaction (SDR) is also one promising DNA nanotechnology, because their process can work without the assist of enzyme under the mild conditions, and the according kinetic rate could be fine-tuned through altering the sequence composition and length of the toehold.[22] Furthermore, the combination of the toehold-mediated SDR and HCR of DNA has been extensively utilized in monitoring DNA,[18] microRNA,[23, 24] biomolecule,[25] protein,[26, 27] and cells [28] due to their excellent performance of specificity, selectivity and no need enzyme for DNA analysis,[22, 29-31] as well as the excellent linear amplification and

superimposition effect. [32] Meanwhile, the integration between DNA amplification strategy and the EBFCs-based self-powered biosensor could be favorable for the performance of the biosensor, as well as the expanded application in the various target detection in many fields.

Single nucleotide polymorphisms (SNPs) have been considered as common genetic variations in human genomes, which are closely associated with various diseases.[33-35] Although substantial methods for SNPs detection have been reported,[36-39] whereas most of them suffered from complicated instruments, tedious experiment procedures, as well as the requirement of labile enzymes and high-cost labels.[36, 40, 41] Thus, it is urgent demand to develop novel simple biosensing platform. In this work, a self-powered biosensor was proposed for the ultrasensitive detection of SNPs via combining EBFC and DNA amplification strategy. And the 18-nucleotide (nt) sequence in the p53 gene comprising the mutation hotspot R273H was chosen to be the target which was named as target18. In this design, the construction of the biocathode was the key factor for biosensing of SNPs. The toehold-mediated hairpin capture probe was immobilized on the AuNPs biocathode through the Au-S bond, in which the toehold and ends could initiate SDR via the specific recognition and hybridization with the target sequence while the open-loop domain could undertake the DNA HCR process with the amplification probe. Subsequently, the EBFCs-based self-powered biosensor was made up of the glucose dehydrogenase (GDH)/N-CNT bioanode and the capture probe/AuNPs biocathode. In the presence of the target sequence (Scheme 1A), the toehold-mediated SDR and successive DNA HCR would promote the generation of a long double-helix chain, which allowed more $[Ru(NH_3)_6]^{3+}$ to reach the biocathde surface due to the electrostatic interaction. Subsequently, $[Ru(NH_3)_6]^{3+}$ could be reduced to $[Ru(NH_3)_6]^{2+}$ by the electrons generated from the bioanode, which produced a high E^{OCV}. In the absence of the target sequence (Scheme 1B), the abovementioned processes could not be accomplished, which resulted in a low E^{OCV}. Consequently, the ultrasensitive detection of SNPs was triumphantly achieved. Moreover, various SNPs could be determined by varying the capture probes on the biocathode. The biosensing strategy was featured with no need for external power source, simplicity, and high sensitivity, which provides a promising protocol for disease diagnostics.

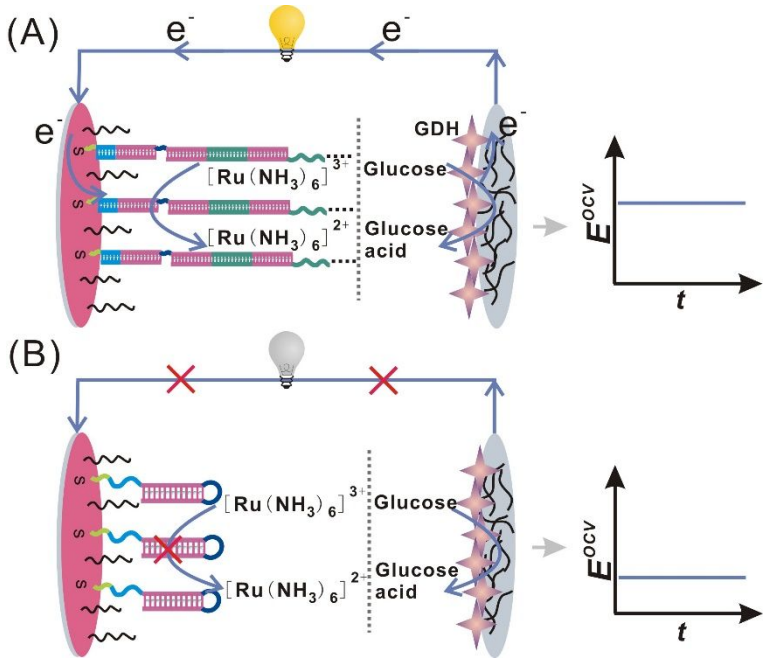

Scheme 1. Schematic illustration of the principle of EBFCs-based self-powered biosensor for SNPs detection based on toehold-mediated DNA amplification strategy

EXPERIMENTAL SECTION

Materials and Reagents. Glucose dehydrogenase from Pseudomonas sp. (NAD), hexaammineruthenium(Ⅲ) chloride ($[Ru(NH_3)_6]^{3+}$, RuHex), *N*-hydroxysuccinimide (NHS), 6-mercapto-1-hexanol (MCH), 1-ethyl-3-(3-dimethyl-aminopropyl) carbodiimide hydrochloride (EDC), and DL-dithiothreitol (DTT) were obtained from Sigma-Aldrich (St. Louis, MO, U.S.A). GelRed was purchased from Biotium. Chloroauric acid ($HAuCl_4 \cdot 4H_2O$) was obtained from Shanghai Chemical Reagent Co., Ltd. (Shanghai, China). AuNPs were prepared through reducing $HAuCl_4$ by sodium citrate.[42] *β*-D-Glucose was purchased from Tokyo Chemical Industry Co., Ltd. (Japan). The HPLC-purified DNA oligonucleotides were purchased from Shanghai Sangon Biotechnology Co., Ltd. (Shanghai, China), and the oligonucleotide sequences used were listed in Table 1. A 20 mM Tris-HCl (pH 7.4) buffer containing 5 mM $MgCl_2$, 5 mM KCl, 137 nM NaCl, and 1 mM DTT was employed as the immobilization buffer (Buffer I). A 100 mM PBS (pH 7.4) buffer containing 0.5 M NaCl was used as mimic-HCR buffer as well as washing buffer (Buffer II). A 10 mM Tris-HCl (pH 7.4) buffer containing 500 μM $[Ru(NH_3)_6]^{3+}$ (Buffer III) and a 100 mM PB solution (pH 7.4) were used as the supporting electrolyte. Ultrapure water (resistivity > 18.2 MΩ cm at 25°C) applied in all the experiments was obtained from a Milli-Q water purification system

(Millipore Corp., Bedford, MA, U.S.A). All other reagents were of analytical grade, which could be used without further purification.

Table 1.The Oligonucleotides Sequences Utilized in This Work[a].

Name	Sequences(5' - 3')
Capture probe	$HS(CH_2)_6$-TCACAAACACGCACCTCAAAGCCATGCTGCTTTGAGGTGC
Capture probe-G	$HS(CH_2)_6$-TCACAAACAGGCACCTCAAAGCCATGCTGCTTTGAGGTGC
Capture probe-A	$HS(CH_2)_6$-TCACAAACAAGCACCTCAAAGCCATGCTGCTTTGAGGTGC
Capture probe-T	$HS(CH_2)_6$-TCACAAACATGCACCTCAAAGCCATGCTGCTTTGAGGTGC
Target 18	GCT TTG AGG TGC GTG TTT
Target 19	GCT TTG AGG TGC GTG TTT G
Target 17	GCT TTG AGG TGC GTG TT
Target 16	GCT TTG AGG TGC GTG T
Mutant A	GCT TTG AGG TGC ATG TTT
Mutant T	GCT TTG AGG TGC TTG TTT
Mutant C	GCT TTG AGG TGC CTG TTT
Mutant D[b]	GCT TTG AGG TGC TGT TT
H1	GTC ATT GCT TTG GCA CCT CAA AGC
H2	CAA AGC AAT GAC GCT TTG AGG TGC

[a]In the capture probes, the toeholds are underlined, and the loops are reded. The mutated bases are highlighted in the box. [b]The mutant type is the deletion of the relative base.

Apparatus and Instrumentation. Transmission electron microscopy (TEM) images were performed and obtained on a HT7700 microscope (Hitachi, Japan) which operated at 100 kV. All electrochemical experiments were carried out on a CHI 660E electrochemical workstation (Shanghai CH Instrument Co., China) at room temperature using a conventional three-electrode system with the constructed biocathode or bioanode as the working electrode, a Ag/AgCl electrode as the reference electrode and a platinum wire as the counter electrode, respectively. The open circuit voltage (E^{OCV}) of EBFC was measured by the connection of the bioanode with the biocathode in the electrolytic cell. The images of gel electrophoresis were scanned by the Gel Doc XR+ Imaging System (BIO-RAD, U.S.A). Electrochemical impedance spectroscopy (EIS) was conducted on an Autolab PGSTAT 302N electrochemical analyzer (Metrohm Autolab, The Netherlands) within a frequency range of 0.1 Hz to 100 kHz and with 2.5 mM $[Fe(CN)_6]^{3-/4-}$ used as the probe.

Preparation and Measurement of the EBFC Biocathode. Upon optimization of varied parameters, the construction process of the EBFC biocathode could be briefly described as follows. First, both H1 and H2 (in Buffer II) solutions were heated to 95°C for 5 min, and then cooled down to room temperature to produce the stem-loop DNA structures for further use. Afterwards, 30 μL of the synthesized AuNPs (50 nM) was dropped onto the surface of ITO electrode (0.5 cm × 0.5 cm) and dried at 37°C for 2 h. Then, 30 μL of capture probe (100 nM) was coated on the aforementioned ITO electrode surface and incubated for 2 h at 37°C. Therewith, MCH (0.05 mM) was cast onto the surface at 37°C for 30 min to block the AuNPs surface to remove the weakly bound capture probes and eliminate the nonspecific adsorption sites. After washing with ultrapure water to get rid of the excessive MCH, the target (100 pM) was injected and kept for 4 h to open the hairpin capture probe and then washed with Buffer II. Subsequently, the modified electrode was immersed in a mixture containing 1 μM H1 and 1 μM H2 for another 2.5 h, followed by washing with Buffer II again for electrochemical measurement. The electrochemical signals were measured with differential pulse voltammetric (DPV), cyclic voltammetric (CV) and linear sweep voltammetric (LSV) measurement by scanning from +0.1 to -0.4 V (versus Ag/AgCl) in 5 mL of Buffer III solution and with quiet time for 5 min.

Electrophoresis Demonstration of DNA Amplification Strategy. The 8% nondenaturating polyacrylamide gel electrophoresis (PAGE) was used in further confirm and characterize the hybrid level of this mimic-HCR amplification strategy. In the PAGE assay, electrophoresis was carried out at 110 V in 1 × TBE (89 mM Tris Borate, 2.0 mM EDTA, pH 8.3) buffer for 50 min at room temperature and stained for 30 min in a 1 × GelRed solution. The imaging of resulting gel was photographed by the gel imaging system under ultraviolet light.

Preparation of GDH/N-CNT Bioanode. 50 μL of 1 mg mL^{-1} N-CNT was dropped on the carbon paper electrode surface (0.5 cm × 0.5 cm) and dried at 37°C. Subsequently, the N-CNT/carbon paper electrode was immersed into a mixture comprised with 1 mg mL^{-1} NHS and 1 mg mL^{-1} EDC for 30 min in order to activate the carboxyl group of N-CNT. After rinsed with ultrapure water for eliminating the excess NHS and EDC, the activated electrode was incubated with 50 μL of GDH solution at 37°C for 30 min to access the GDH/N-CNT bioanode. GDH could be immobilized on

the electrode by the condensation reaction of the amino groups in enzymes with the carboxyl groups on N-CNTs.

Fabrication and Measurement of EBFCs-Based Self-Powered Biosensing Platform. An EBFCs-based self-powered biosensor was performed in a two-compartment-cell configuration by exploiting the fabricated biocathode and bioanode at room temperature. The area of working electrode was 0.25 cm^2 (0.5 cm × 0.5 cm). The bioanode compartment was filled with 15 mL of 100 mM PB (pH 7.4) solution containing 5 mM glucose, while the biocathode compartment was saturated with 15 mL of Buffer III. The E^{OCV} of the EBFC was carried out on CHI 660E electrochemical workstation in a two-compartment-cell configuration with quiet time for 5 min.

Cell Culture and Cell Lysis. Human cervical cancer cells (HeLa cells) were seeded in DMEM (Dulbecco's Modified Eagle Medium, Gibco, Grand Island, NY, U.S.A.) supplemented with 10% (v/v) fetal bovine serum (FBS), 100 μg mL^{-1} streptomycin, and 100 μg mL^{-1} penicillin in a 5% CO_2 37°C incubator. Then, incubated HeLa cells were collected by trypsinization and centrifugation, washed with PBS, following that the cell number was counted by hemocytometer. Meanwhile, The cells were resuspended in RIPA cell lysis solution at a concentration of 1.0×10^6 cells/mL, incubated for 5 min, and then centrifuged at 12 000 rpm for 5 min to get the supernatant liquid for later use.

RESULTS AND DISCUSSION

Design and Characterization of the Biocathode. The performance of biocathode has a vital effect for the achievement of selective and sensitive detection for SNPs, thus the biocathode was rationally and elaborately designed (Scheme 2). Herein, AuNPs featured with uniform morphology (TEM image in Figure S1) were chosen as the substrate materials owing to their inherent merits of excellent conductivity and good biocompatibility. Besides, the sulfhydryl group-modified toehold-mediated capture probe was immobilized onto the AuNPs/ITO electrode through Au-S bonds. In the capture probe, the sequence of the external toehold and linked stem strand was completely complementary to the target sequence, and the stem sequence at the 3′ end was completely complementary to the amplification probes Hairpin 1 (H1) and Hairpin 2 (H2), while the loop sequence is not complementary to any sequence. Once the target sequence was introduced, the SDR was initiated

by the hybridization between the target and the toehold domain, and completed through the migration and exposure of the stem strand at the 3′ end. Afterwards, the exposed single strand (the HCR initiator) hybridized with the amplification probes H1 and H2 for the sake of improving the output signals. In this process, H1 was first opened via the recognition of the initiator with the sticky end of H1 and the succeeding SDR with the purple fragment of H1, while H2 was subsequently unfolded by the identification of newly exposed fragment of H1 with the sticky end of H2 as well as the following SDR with the green fragment of H2, which resulted in the formation of a long double-helix by the cyclic HCR. When the treated electrode was immersed in the $[Ru(NH_3)_6]^{3+}$ solution, because of the excellent electrochemical activity of the $[Ru(NH_3)_6]^{3+}$, the more positive charged $[Ru(NH_3)_6]^{3+}$ were captured via electrostatic interaction, the higher electrochemical signals were obtained. By contrast, in the presence of the mutant sequence, the SDR process was obstructed, since the single-base mismatch at the 3′ end of the external toehold significantly restrained the hybridization between the capture probe and the mutant sequence. In this process, although partly amplification hairpin probes could also hybridize with each other owing to their base complementary, they could not achieve successive HCR processes on the electrode surface due to its unbound state. Accordingly, it is almost impossible to accomplish the SDR and successive HCR processes on the electrode without the trigger of target sequence, the electrochemical signal decreased obviously on account of the electron transfer process hindered on the electrode surface.

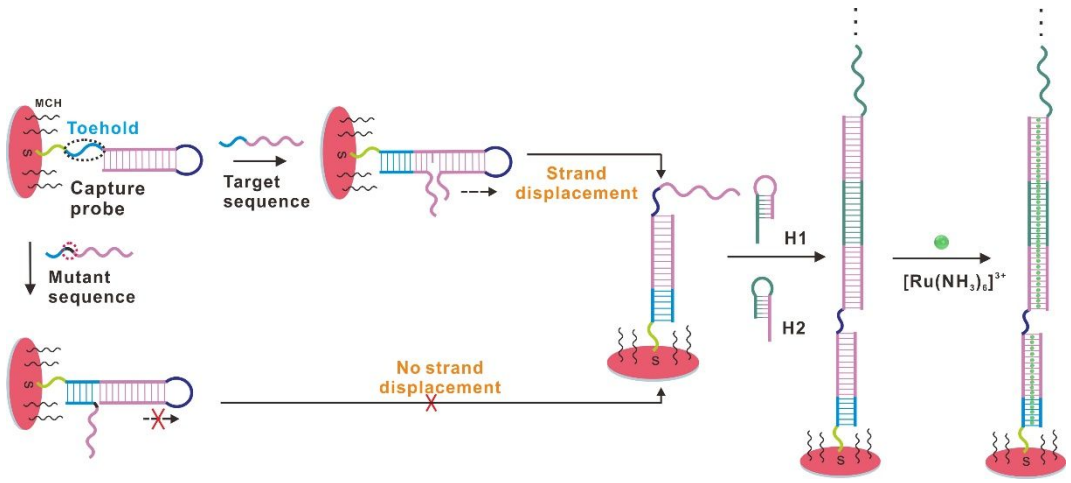

Scheme 2. Schematic illustration of the principle of the biocathode of EBFC-based self-powered biosensing platform for SNPs analysis.

To verify the aforementioned protocol, the capture probe and target 18 were selected as examples to evaluate the performance of biocathode. Firstly, gel electrophoresis was applied to characterize the amplification by toehold-mediated SDR and HCR sequence (Figure 1A). All the basic DNA structures including CP (lane 1), target 18 (lane 2), Mutant C (lane 3), H1 (lane 9) and H2 (lane 10), displayed a narrow and single electrophoresis band on both gel board, illustrating no secondary structure in the rationally designed DNA sequence. When CP incubated with target 18 or mutant C for 2 h (lanes 4 and 5), a new band was showed in lane 4 on both gel board, validating that the CP@target double strands was formed. However, there was no new band displayed in lane 5, mainly because the toehold-mediated strand displacement was prevented by the single base mismatch. When both H1and H2 co-existed, they would partially hybridize each other to form the extended DNA complex while part of unreacted species still existed (Lane 8). Once initiator strands existed, H1 and H2 were opened completely, resulting in the unreacted species almost disappeared, and suggesting the HCR process was initiated successfully (Lane 6). Based on the successful HCR, DPV and CV measurements were implemented to explore the response of the electron acceptor at the biocathode. In our design, $[Ru(NH_3)_6]^{3+}$ was selected as the signal molecule due to its capability of inserting DNA double strands via electrostatic interaction as well as accepting electrons from the electrode. As shown in Figure 1B and 1C, the peak current value was weak only in the presence of capture probe (curve a). When the capture probe incubated with target 18 or mutant C, the peak current values slightly increased (curve b and c) because not so much $[Ru(NH_3)_6]^{3+}$ was bound. Similarly, the electrode modified with mutant C further incubated with hairpin probes H1 and H2, the signal increased to some extent (curve d) because the part of hybridized amplification probes with $[Ru(NH_3)_6]^{3+}$ was attached to the electrode surface. However, once the electrode modified with target 18 further incubated with H1 and H2, the signal remarkably increased (curve e), because numerous $[Ru(NH_3)_6]^{3+}$ trapped in double strands was transferred electrons to the electrode by DNA chains, which indicated that the amplification effect was effective and efficient by toehold-mediated SDR and HCR processes. Meanwhile, the same tendency could also be obtained from Figure 1C, only the electrode incubated with target 18 could achieve HCR process in the present of H1 and H2, so that numerous positive charged $[Ru(NH_3)_6]^{3+}$ were inserted into the double strands and resulting in the remarkably increased electrochemical signal (curve e).

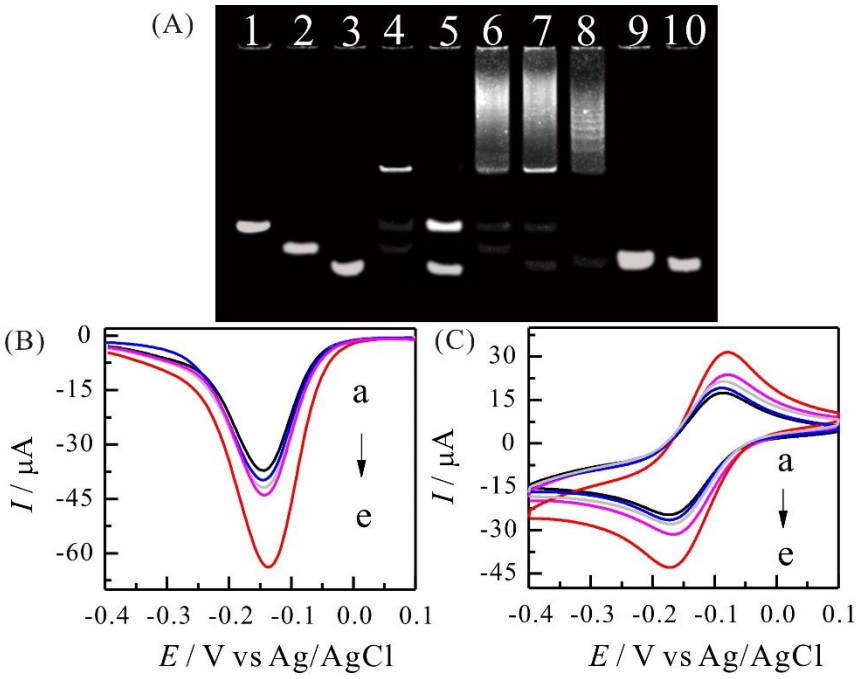

Figure 1. (A) SG-stained 8% polyacrylamide gel electrophoresis (PAGE) image. Lane 1, CP; lane 2, target 18; lane 3, Mutant C; lane 4, CP+target 18; lane 5, CP+Mutant C; lane 6, CP+target 18+H1+H2; lane 7, CP+Mutant C+H1+H2; lane 8, H1+H2; lane 9 , H1; lane 10, H2 (all the samples were mixed and incubated at 37℃ for 2 h). DPV (B) and CV (C) responses of the biocathode to DNA hybrid level (a-e: CP, CP+Mutant C, CP+target 18, CP+Mutant C+H1+H2, CP+target 18+H1+H2). The concentrations of capture probe, target 18/Mutant C and H1/H2 were 100 nM, 100 pM and 1 μM, respectively.

Optimization of Assay Conditions. In order to achieve the excellent performance of EBFCs-based self-powered biosensing platform, the incubation times between target 18 and capture probe as well as between the functionalized electrode and H1+H2 were optimized by DPV measurements. As shown in Figure S2A, the peak current enhanced over time due to the process of target 18 hybridized with capture probe required adequate reaction time. Further, the peak current kept unchanged after 4.0 h, demonstrating that the capture probe modified on the electrode was completely opened by the target 18. Thus, 4.0 h was preferable in the reaction system. Likewise, the peak current also increased with time before 2.5 h, the maximum peak current at 2.5 h suggesting that the functionalized electrode was sufficiently reacted with H1+H2 at this time. Therefore, 2.5 h was adequate for the incubation time (Figure S2B).

Electrochemical Characterization of Biocathode. As the crucial component of the EBFCs-based self-powered biosensor, the electrochemical properties of biocathode were very important. As shown in Figure 2, DPV measurements were performed to examine the SNPs. The hairpin capture probes would completely hybrid with their targets, in which the bases at the "X" and "Y" points could be adenine (A), thymine (T), cytosine (C), or guanine (G), so that the hairpin was opened and exposed the newly single strand to trigger the HCR to increase the insertion rate of $[Ru(NH_3)_6]^{3+}$. The above mentioned consequences were consistent with the DPV signals. And we could confirm that the monitoring of SNPs would be accomplished through the target-mediated HCR at the biocathode. Meanwhile, except the single-base mutant sequences, the biosensing platform could also distinguish the target 18 from random sequences. As depicted in Figure S3, target 18 and random sequences were treated with the same conditions. Compared with that of the blank (curve a), the peak currents of random sequences (curve b-e) only increased to some extent due to the slightly adsorption on the electrode. However, the peak current of target 18 functionalized electrode (curve f) remarkably increased, demonstrating that the toehold-mediated SDR served as the precondition for the following HCR process to accomplish signal amplification. On these basis, it was further deducted that the biocathode of EBFCs-based self-powered biosensing platform could efficiently detect the target 18.

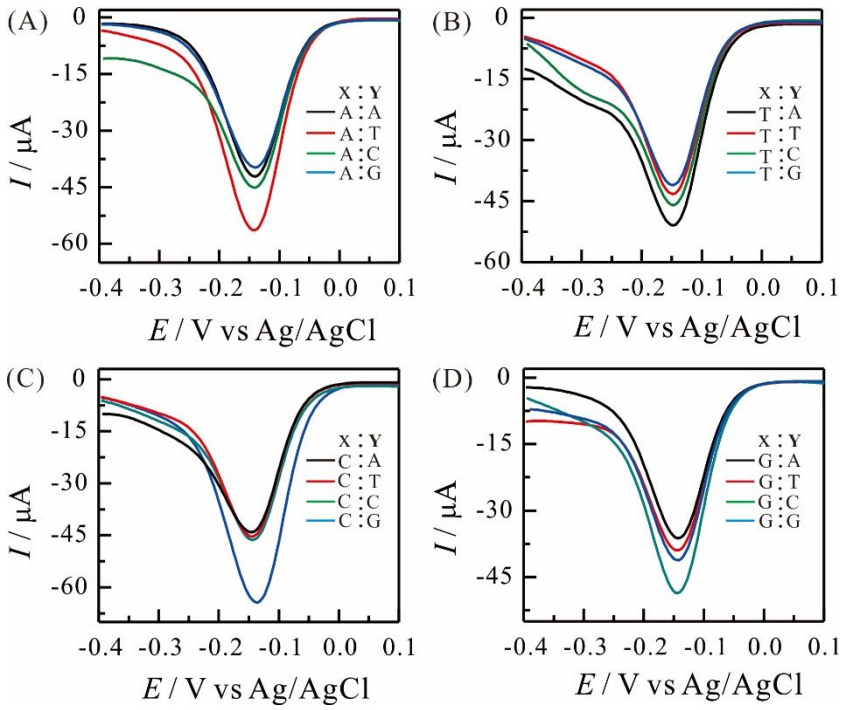

Figure 2. DPV responses of the self-powered biosensing platform obtained using the capture probe as the scaffold (X: (A) A, (B) T, (C) C, and (D) G) hybridized with target (Y: A, T, C, G) to achieve the HCR process. The concentrations of capture probe, target, H1/H2 were 100 nM, 100 pM, 1 μM, respectively.

Characterization of the Bioanode. The bioanode of EBFC not only functioned as the electron generator but also played a crucial effect during the construction of self-powered biosensing platform. Herein, electrochemical impedance spectroscopy (EIS) was employed to explore the charge separation effect in the bioanode fabrication process. Figure S4 showed that N-CNT modified carbon paper (curve a) exhibited a smaller electron-transfer resistance (R_{et}) value than the bare carbon paper (curve b), because of the excellent conductivity of N-CNT. Furthermore, the R_{et} obviously increased when NAD^+-dependent GDH was modified, owing to the huge steric hindrance effect of proteins (curve c). The results strongly affirmed that the functionalized bioanode was successfully constructed. In addition, the N-CNT functioned bioanode was beneficial to decrease the overpotential of NADH oxidation, which made it easier for oxidizing NADH to NAD^+ to realize the recycle of NAD^+.[43] Just as expected, the potential of NADH was only at -0.05 V (Figure 3A). Afterwards, the oxidation current further raised with the increasing NADH concentrations, illustrating that the cofactor NAD^+ could be efficiently recycled with the aid of N-CNT. Meanwhile, the oxidation of glucose would operate on the GDH/N-CNT bioanode. When the glucose was added, the oxidation current intensity increased and was proportional to the concentration, indicating the GDH/N-CNT bioanode could efficiently catalyze the glucose oxidation (Figure 3B). Hence, the abovementioned results laid the foundation for structuring an EBFC-based self-powered biosensing platform with high-performance.

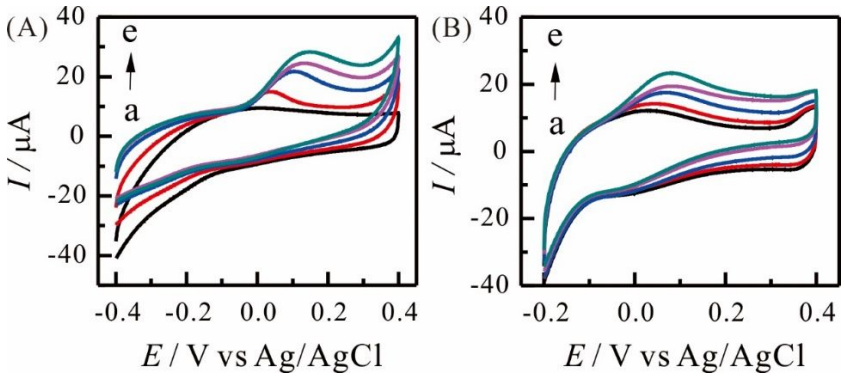

Figure 3. (A) CVs of GDH/N-CNT bioanode in the absence (a) and the presence of 1 mM (b), 2 mM (c), 3 mM (d), and 4 mM (e) NADH in PB (10 mM, pH 7.4). (B) CVs of the GDH/N-CNT bioanode in PB (10 mM, pH 7.4) containing 1mM NADH and 2 mM NAD^+, in the absence (a) and presence of 1 mM (b), 2 mM (c), 3 mM (d), and 4 mM (e) glucose. υ = 50 mV s^{-1}.

Feasibility of EBFCs-Based Self-Powered Biosensing Platform. The EBFCs-based self-powered biosensing platform was composed of HCR/AuNPs biocathode and GDH/N-CNT bioanode. To further verify the feasibility of the fabricated self-powered biosensing platform for SNPs, the Mutant C and target 18 were chosen as the example to conduct OCP characterization. From Figure 4, the E^{OCV} value of the electrode only modified with capture probe was 0.115 V (curve a). And after introducing target 18 and mutant C, the E^{OCV} values were 0.15 V and 0.145 V, respectively (curve c and b) because not so much $[Ru(NH_3)_6]^{3+}$ was bound. What's more, after the functionalized electrodes were immersed into the H1 and H2 mixture solution, the E^{OCV} value of mutant C modified electrode increased slightly (curve e) due to the slightly adsorption on the electrode. However, the E^{OCV} value of target 18 modified electrode distinctly increased and reach up to 0.27 V (curve f), demonstrating that the amplification effect through HCR should take toehold-mediated SDR as a prerequisite.

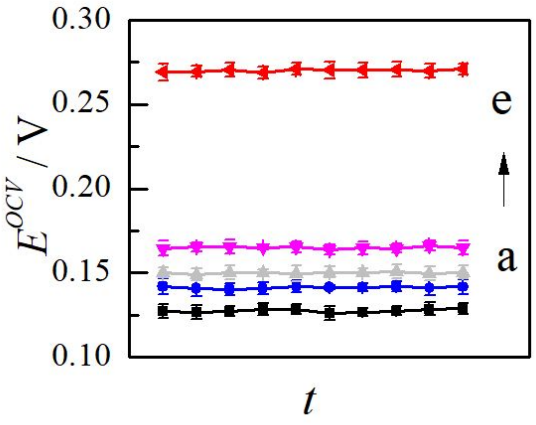

Figure 4. OCP responses of the proposed EBFCs-based self-powered biosensing platform to DNA hybrid level (a-e: CP, CP+Mutant C, CP+target 18, CP+Mutant C+H1+H2, CP+target 18+H1+H2). The concentrations of capture probe, target 18/Mutant C, H1/H2 were 100 nM, 100 pM, 1 μM, respectively.

EBFCs-Based Self-Powered Biosensing Platform for SNPs. To expand the application of our biosensing platform in identifying more general single-nucleotide mismatches, a new duplex was designed, which was composed of a hairpin capture probe strand (CP) and a target strand (target) (Table 1). For duplex CP/target, the bases at the "X" and "Y" points could be adenine (A), thymine (T), cytosine (C), or guanine (G). 16 possible base-pair combinations of XY duplexes were obtained by respectively varying the bases at the X and Y points in CP and target, which covered all varieties of single-nucleotide mismatches at the mutation point. The newly generated DNA duplexes were utilized to unfold the hairpin capture probe and further provide the exposed single strand to initiate the hybridization chain reaction, and the corresponding OCP responses were shown in Figure 5. When the base at the X point of CP was complementary to the one at the Y point of target [(A) A:T; (B) T:A; (C) C:G; (D) G:C], the corresponding DNA duplex was obtained by toehold-mediated strand displacement reaction, which the highest OCP value relative to those for the other three situations with the single-nucleotide mismatch at the X:Y point. The results demonstrated the feasibility of identifying different kinds of single-nucleotide mutations using the self-powered EBFC biosensing platform based on toehold-mediated SDR and HCR processes.

Selectivity. The selectivity of the self-powered biosensing platform is a vital parameter for the detection of SNPs. The relationships between the E^{OCV} value and target 18 or random sequences based on toehold-mediated HCR were also investigated to affirm the specificity of this biosensing platform. As it can be deduced from Figure S5, only the perfectly matched target DNA (curve f) provided a significantly different OCP signal from the blank and random sequence (curve b-e), producing a high E^{OCV} value. On the one hand, the toehold-mediated SDR always gradually proceeded, and the impending strand displacement was greatly prevented by the mismatch between the random sequences and the capture probe at the 3′ end of the external toehold. On the other hand, the hairpin capture probe, owing to its excellent thermal stability, only hybridized with a totally complementary ssDNA (such as target 18) to form a more stable duplex, whereas the random sequences were insufficient to unfold the capture probe. According to the above arguments, only when the capture probe corresponded with target, the strand displacement could be triggered, thereby accomplishing the signal amplification by HCR. These results further confirmed that the above constructed biosensing platform could effective and selective identified SNPs.

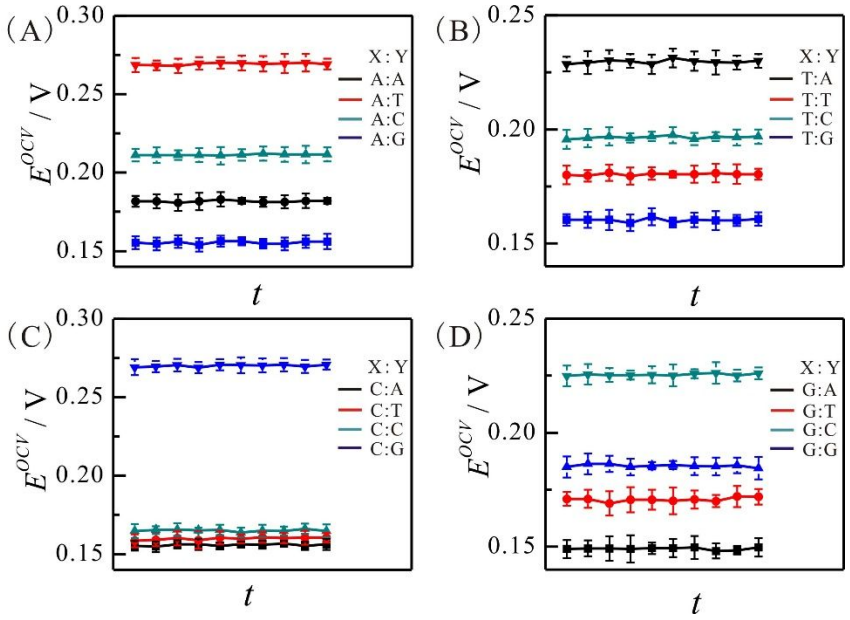

Figure 5. OCP responses of the self-powered biosensing platform obtained by using the capture probe as the scaffold (X: (A) A, (B) T, (C) C, and (D) G) hybridized with target (Y: A, T, C, G) to achieve the HCR. The concentrations of capture probe, target and H1/H2 were 100 nM, 100 pM and 1 μM, respectively.

EBFCs-Based Self-Powered Biosensing Platform for Target 18 Detection. Under the optimal experimental conditions, the as-proposed self-powered biosensing platform was also utilized to detect target 18. As expected, the E^{OCV} gradually increased with the increasing target concentrations which ranged from 0 to 10 nM (Figure 6A). Furthermore, a linear relationship was presented between E^{OCV} and the logarithm of target 18 concentration in the range of 0.1 to 500 pM, with a linear equation of $E^{OCV} = 0.171 + 0.042 \log c_{\text{target 18}}$ (correlation coefficient $R^2 = 0.9940$). It should also be noted that the as-proposed self-powered biosensing platform displayed outstanding performance, with a low detection limit of 20 aM (S/N = 3), being comparable or even superior to those of the reported methods (Table S1).

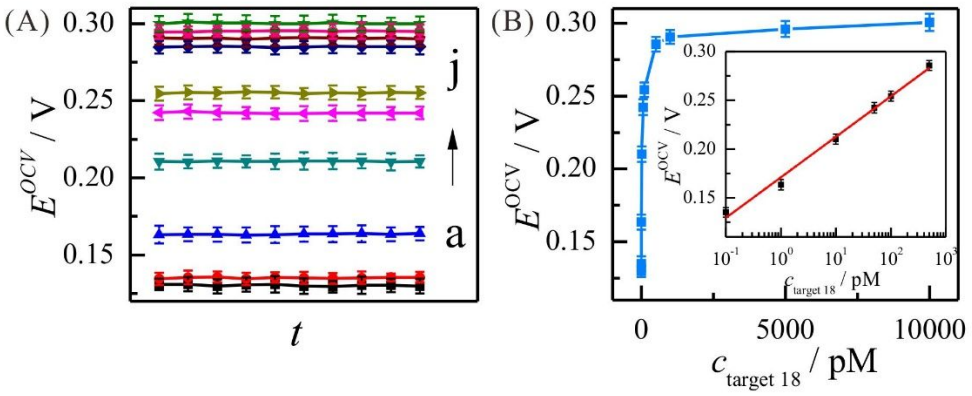

Figure 6. (A) E^{OCV} of the as-proposed biosensing platform under different target 18 concentrations (from a to j: 0, 0.1, 1, 10, 50, 100, 500, 1000, 5000, 10000 pM). (B) E^{OCV} values vs target 18 concentration. Inset shows the linear relationship between E^{OCV} values and the logarithm of target 18 concentration from 0.1 to 500 pM. Error bars represent the standard deviation of independent measurements of three self-powered biosensing platform.

Target 18 Detection in Cell Lysates. In order to confirm the feasibility of applying the as-proposed biosensing platform for real samples, the cell lysate extracted from HeLa cells was employed. Initially, the targets of different concentrations were added into the 10% HeLa cells lysates and analyzed by the self-powered biosensing platform. Table S2 shows that the recoveries of target 18 were 97.6%-106.5%, the RSDs were 3.27%-4.49% (n = 6). The mentioned preliminary results illustrated that the as-proposed self-powered biosensing platform would enable to apply to SNPs detection in biological samples.

CONCLUSIONS

A new self-powered biosensing platform for the ultrasensitive and selective detection of SNPs via integration of EBFCs and DNA amplification strategy was proposed. Especially, the ingenious design of the integration with the toehold-mediated SDR and DNA HCR reaction efficiently enabled the high sensitivity of the as-prepared biosensor. Furthermore, the as-proposed self-powered biosensor also produced significant discrimination capability to the p53 gene fragments against random sequences. More importantly, the presence of target sequence could make the signal (E^{OCV}) of the as-proposed biosensor significantly elevated, which could reduce the interference of background. The work not only provides a new insight to solve the limitations of lower sensitivity but also laid a great foundation for disease diagnostics as a powerful tool.

ASSOCIATED CONTENT

Supporting Information

Additional information as noted in the text. TEM image of AuNPs; The experimental condition optimization of the proposed strategy; DPV responses of the biocathode in different conditions; EIS of the bioanode; OCP responses of the self-powered EBFC biosensing platform; Measurement of target 18 added to the HeLa cell lysates by means of standard addition; Comparison of target 18 detection performance between our and other reported methods.

AUTHOR INFORMATION

Corresponding Author

*E-mail: lifeng@qau.edu.cn (F. Li)

Tel/Fax: (86) 532-86080855

Notes

The authors declare no competing financial interest.

ACKNOWLEDGMENTS

We gratefully appreciate the financial support from the National Natural Science Foundation of China (21605092, 21775083 and 21775082), Shandong Provincial Natural Science Foundation, (ZR2019YQ23), the Research Foundation for Distinguished Scholars of Qingdao Agricultural University (663-1117002), and the Special Foundation for Taishan Scholar of Shandong Province (No. ts201511052).

REFERENCES

1. Zhao, C. E., Gai, P. P., Song, R. B., Chen, Y., Zhang, J. R., Zhu, J. J., *Nanostructured material-based biofuel cells: recent advances and future prospects*. *Chem. Soc. Rev.* 2017, *46*. 1545-1564.

2. Szczupak, A., Halámek, J., Halámková, L., Bocharova, V., Alfonta, L., Katz, E., *Living battery – biofuel cells operating in vivo in clams*. *Energy Environ. Sci.* 2012, *5*. 8891-8895.

3. Grattieri, M., Minteer, S. D., *Self-Powered Biosensors*. *ACS Sens.* 2017, *3*. 44-53.

4. Zhou, M., Dong, S. J., *Bioelectrochemical Interface Engineering: Toward the Fabrication of Electrochemical Biosensors, Biofuel Cells, and Self-Powered Logic Biosensors*. *Acc. Chem. Res.* 2011, *44*. 1232-1243.

5. Zhou, M., *Recent Progress on the Development of Biofuel Cells for Self-Powered Electrochemical Biosensing and Logic Biosensing: A Review*. *Electroanalysis* 2015, *27*. 1786-1810.

6. Pang, X., Cui, C., Su, M., Wang, Y., Wei, Q., Tan, W. H., *Construction of self-powered cytosensing device based on ZnO nanodisks@g-C_3N_4 quantum dots and application in the detection of CCRF-CEM cells*. *Nano Energy* 2018, *46*. 101-109.

7. Gai, P. P., Ji, Y. S., Wang, W. J., Song, R. B., Zhu, C., Chen, Y., Zhang, J. R., Zhu, J. J., *Ultrasensitive self-powered cytosensor*. *Nano Energy* 2016, *19*. 541-549.

8. Gai, P. P., Song, R. B., Zhu, C., Ji Y. S., Wang, W. J. Zhang, J.R., Zhu., J. J., *Ultrasensitive self-powered cytosensors based on exogenous redox-free enzyme biofuel cells as point-of-care tools for early cancer diagnosis*. *Chem. Commun.* 2015. 16763-16766.

9. Gu, C. C., Gai, P. P., Hou, T., Li, H. Y., Xue, C. H., Li, F., *Enzymatic Fuel Cell-Based Self-Powered Homogeneous Immunosensing Platform via Target-Induced Glucose Release: An Appealing Alternative Strategy for Turn-On Melamine Assay*. *ACS Appl. Mater. Interfaces* 2017, *9*. 35721-35728.

10. Cheng, J., Han, Y., Deng, L., Guo, S. J., *Carbon nanotube-bilirubin oxidase bioconjugate as a new biofuel cell label for self-powered immunosensor*. *Anal. Chem.* 2014, *86*. 11782-11788.

11. Wang, Y., Ge, L., Wang, P., Yan, M., Yu, J., Ge, S., *A three-dimensional origami-based immuno-biofuel cell for self-powered, low-cost, and sensitive point-of-care testing*. *Chem. Commun.* 2014, *50*. 1947-1949.

12. Jung, Y. K., Kim, K. N., Baik, J. M., Kim, B. S., *Self-powered triboelectric aptasensor for label-free highly specific thrombin detection*. *Nano Energy* 2016, *30*. 77-83.

13. Lin, Z. H., Cheng, G., Wu, W. Z., Ken C. Prade, LinWang, Z., *Dual-Mode Triboelectric Nanogenerator for Harvesting Water Energy and as a Self-Powered Ethanol Nanosensor*. *ACS Nano* 2014, *8*. 6440-6448.

14. Bai, L., Jin, L., Han, L., Dong, S. J., *Self-powered fluorescence controlled switch systems based on biofuel cells*. *Energy Environ. Sci.* 2013, *6*. 3015-3021.

15. Yan, K., Yang, Y., Zhu, Y., Zhang, J., *Highly Selective Self-Powered Sensing Platform for p-Nitrophenol Detection Constructed with a Photocathode-Based Photocatalytic Fuel Cell*. *Anal. Chem.* 2017, *89*. 8599-8603.

16. Gai, P. P., Gu, C. C., Hou, T., Li, F., *Ultrasensitive Self-Powered Aptasensor Based on Enzyme Biofuel Cell and DNA Bioconjugate: A Facile and Powerful Tool for Antibiotic Residue Detection*. *Anal. Chem.* 2017, *89*. 2163-2169.

17. Zhou, M., Wang, J., *Biofuel Cells for Self-Powered Electrochemical Biosensing and Logic Biosensing: A Review*. *Electroanalysis* 2012, *24*. 197-209.

18. Xu, G., Zhao, H., Reboud, J., Cooper, J. M., *Cycling of Rational Hybridization Chain Reaction To Enable Enzyme-Free DNA-Based Clinical Diagnosis*. *ACS Nano* 2018, *12*. 7213-7219.

19. Yue, S. Z., Song, X. Y., Song, W. L ., Bi, S., *An enzyme-free molecular catalytic device:dynamically self-assembled DNA dendrimers for in situ imaging of microRNAs in live cells*. *Chem. Sci.* 2019, *10*. 1651-1658.

20. Bi, S., Yue, S. Z., Zhang, S. S., *Hybridization chain reaction: a versatile molecular tool for biosensing, bioimaging, and biomedicine*. *Chem. Soc. Rev.* 2017, *46*. 4281-4298.

21. Li, Y. F., Yue, X. Z., Qi, H. J., Ding, C. F., Song, W. L., Bi, S., *Target-triggered dynamic hairpin assembly for signal amplification of microRNA and oncogenes and its application in live-cell imaging*. *Chem. Commun.* 2019, *55*. 4103-4106.

22. Gao, Z. F., Ling, Y., Lu, L., Chen, N. Y., Luo, H. Q., Li, N. B., *Detection of single-nucleotide polymorphisms using an ON-OFF switching of regenerated biosensor based on a locked nucleic acid-integrated and toehold-mediated strand displacement reaction*. *Anal. Chem.* 2014, *86*. 2543-2548.

23. Liu, L., Liu, J. W., Wu, H., Wang, X. N., Yu, R. Q., Jiang, J. H., *Branched Hybridization Chain Reaction Circuit for Ultrasensitive Localizable Imaging of mRNA in Living Cells*. *Anal. Chem.* 2018, *90*. 1502-1505.

24. Ge, Z., Lin, M., Wang, P., Pei, H., Yan, J., Shi, J., Huang, Q., He, D., Fan, C., Zuo, X., *Hybridization chain reaction amplification of microRNA detection with a tetrahedral DNA nanostructure-based electrochemical biosensor*. *Anal. Chem.* 2014, *86*. 2124-2130.

25. Xu, Q., Zhu, G., Zhang, C. Y., *Homogeneous bioluminescence detection of biomolecules using target-triggered hybridization chain reaction-mediated ligation without luciferase label*. *Anal. Chem.* 2013, *85*. 6915-6921.

26. Li, J., Liu, S., Sun, L., Li, W., Zhang, S. Y., Yang, S., Li, J., Yang, H. H., *Amplified Visualization of Protein-Specific Glycosylation in Zebrafish via Proximity-Induced Hybridization Chain Reaction*. *J. Am. Chem. Soc.* 2018, *140*. 16589-16595.

27. Zhang, B., Liu, B., Tang, D., Niessner, R., Chen, G., Knopp, D., *DNA-based hybridization chain reaction for amplified bioelectronic signal and ultrasensitive detection of proteins*. *Anal. Chem.* 2012, *84*. 5392-5399.

28. Choi, J., Love, K. R., Gong, Y., Gierahn, T. M., Love, J. C., *Immuno-hybridization chain reaction for enhancing detection of individual cytokine-secreting human peripheral mononuclear cells*. *Anal. Chem.* 2011, *83*. 6890-6895.

29. Kong, J., Zhu, J., Keyser, U. F., *Single molecule based SNP detection using designed DNA carriers and solid-state nanopores*. *Chem. Commun.* 2016, *53*. 436-439.

30. Wang, W. J., Li, J. J., Rui, K., Gai, P. P., Zhang, J. R., Zhu, J. J., *Sensitive electrochemical detection of telomerase activity using spherical nucleic acids gold nanoparticles triggered mimic-hybridization chain reaction enzyme-free dual signal amplification*. *Anal. Chem.* 2015, *87*. 3019-3026.

31. Wang, D., Tang, W., Wu, X., Wang, X., Chen, G., Chen, Q., Li, N., Liu, F., *Highly selective detection of single-nucleotide polymorphisms using a quartz crystal microbalance biosensor based on the toehold-mediated strand displacement reaction*. *Anal. Chem.* 2012, *84*. 7008-7014.

32. Zhang, H., Dong, H., Yang, G., Chen, H., Cai, C., *Sensitive Electrochemical Detection of Human Methyltransferase Based on a Dual Signal Amplification Strategy Coupling Gold Nanoparticle-DNA Complexes with Ru(III) Redox Recycling*. *Anal. Chem.* 2016, *88*. 11108-11114.

33. Suh, Y., Vijg, J., *SNP discovery in associating genetic variation with human disease phenotypes*. *Mutat. Res.* 2005, *573*. 41-53.

34. Figl, A., Scherer, D., Nagore, E., Bermejo, J. L., Dickes, E., Thirumaran, R. K., Gast, A., Hemminki, K., Kumar, R., Schadendorf, D., *Single nucleotide polymorphisms in DNA repair genes XRCC1 and APEX1 in progression and survival of primary cutaneous melanoma patients*. *Mutat. Res.* 2009, *661*. 78-84.

35. Zhang, D., Ma, J., Brismar, K., Efendic, S., Gu, H. F., *A single nucleotide polymorphism alters the sequence of SP1 binding site in the adiponectin promoter region and is associated with diabetic nephropathy among type 1 diabetic patients in the Genetics of Kidneys in Diabetes Study*. *J. diabetes complications* 2009, *23*. 265-272.

36. Huang, C. J., Lin, Z. E., Yang, Y. S., Chan, H. W., Chen, W. Y., *Neutralized chimeric DNA probe for detection of single nucleotide polymorphism on surface plasmon resonance biosensor*. *Biosens. Bioelectron.* 2018, *99*. 170-175.

37. Feng, Y., Sun, F., Wang, N., Lei, J., Ju, H., *$Ru(bpy)_3^{2+}$ Incorporated Luminescent Polymer Dots: Double-Enhanced Electrochemiluminescence for Detection of Single-Nucleotide Polymorphism*. *Anal. Chem.* 2017, *89*. 7659-7666.

38. Zhang, X. R., Zhang, Y., Chen, F. T., Li, Y., Zhang, S. S., *Visual detection of single-nucleotide polymorphisms and DNA methyltransferase based on cation-exchange of CuS nanoparticles and click*

chemistry of functionalized gold nanoparticles. *Chem. Commun.* 2016, *52*. 13261-13264.

39. Guo, W. W., Yuan, J. P., Dong, Q. Z., Wang, E. K., *Highly Sequence-Dependent Formation of Fluorescent Silver Nanoclusters in Hybridized DNA Duplexes for Single Nucleotide Mutation Identification*. *J. Am. Chem. Soc.* 2010, *132*. 932-934.

40. Yang, A. H., Hsieh, K., Patterson, A. S., Ferguson, B. S., Eisenstein, M., Plaxco, K. W., Soh, H. T., *Accurate zygote-specific discrimination of single-nucleotide polymorphisms using microfluidic electrochemical DNA melting curves*. *Angew. Chem. Int. Ed.* 2014, *53*. 3163-3167.

41. Wei, B., Zhang, T., Ou, X., Li, X., Lou, X., Xia, F., *Stereochemistry-Guided DNA Probe for Single Nucleotide Polymorphisms Analysis*. *ACS Appl. Mater. Interfaces* 2016, *8*. 15911-15916.

42. Li, F., Feng, Y., Dong, P., Tang, B., *Gold nanoparticles modified electrode via a mercapto-diazoaminobenzene monolayer and its development in DNA electrochemical biosensor*. *Biosens. Bioelectron.* 2010, *25*. 2084-2088.

43. Goran, J. M., Favela, C. A., Stevenson, K. J., *Electrochemical Oxidation of Dihydronicotinamide Adenine Dinucleotide at Nitrogen-Doped Carbon Nanotube Electrodes. Anal. Chem.* 2013, *85*, 9135-9141.

Only For TOC

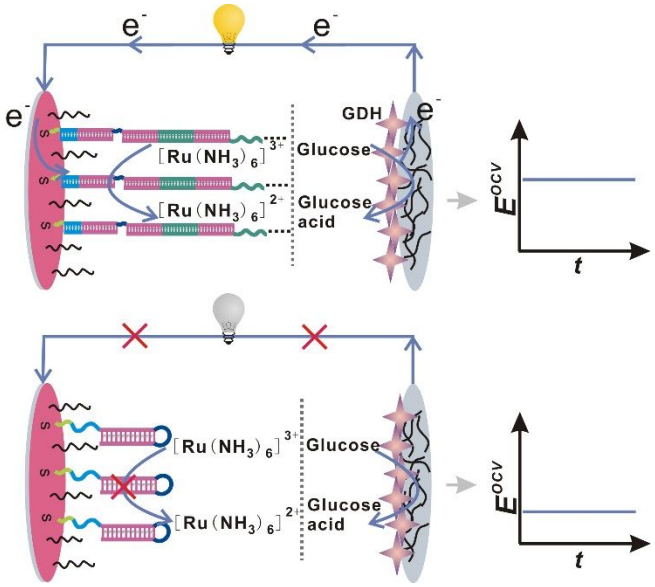
e⁻
e⁻
e⁻
e⁻
GDH
[Ru(NH3)6]3+
[Ru(NH3)6]2+
Glucose
Glucose acid
EOCV
t
[Ru(NH3)6]3+
[Ru(NH3)6]2+
Glucose
Glucose acid
EOCV
t